

Differential subcellular localization of X-linked inhibitor of apoptosis protein (XIAP) modulates drug resistance, cell growth and prognosis in breast cancer

Deborah Delbue¹, Bruna dos Santos Mendonça¹, Marcela C. Robaina¹, Pedro Ivo Lucena³, João P.B. Viola², Caio A.B. Oliveira³, Felipe R. Teixeira³, Raquel C. Maia¹, Gabriela Nestal de Moraes¹

¹Laboratório de Hemato-Oncologia Celular e Molecular; Programa de Hemato-Oncologia Molecular; Instituto Nacional de Câncer (INCA). Rio de Janeiro (RJ), Brazil. ²Programa de Imunologia e Biologia Tumoral, INCA, RJ, Brazil. ³Departamento de Genética e Evolução, Universidade Federal de São Carlos, SP, Brazil.

Evasion from apoptosis is one of the hallmarks of cancer. X-linked inhibitor of apoptosis protein (XIAP) is known to modulate apoptosis by inhibiting caspases and ubiquitinating target proteins. XIAP is mainly found at the cytoplasm, but recent data link nuclear XIAP to poor prognosis in breast cancer. Here, we generated a mutant form of XIAP with a nuclear localization signal (XIAP^{NLS-C-term}) and investigated the oncogenic mechanisms associated with nuclear XIAP in breast cancer. We show that cells overexpressing XIAP^{ΔRING} (RING deletion) and XIAP^{NLS-C-term} exhibited XIAP nuclear localization more abundantly than XIAP^{wild-type}, as analyzed by confocal microscopy, cell fractionation and immunoblotting (Figures 1 and 2). Remarkably, overexpression of XIAP^{NLS-C-term}, but not XIAP^{ΔRING}, induced chemoresistance (Figure 3) and cell growth (Figure 4), as assessed by cell counting, flow cytometry, clonogenic, MTT and crystal violet assays. Interestingly, Survivin and cIAP1 expression, as well as NFκB activity, were not associated with RING-mediated XIAP oncogenic effects (Figure 5). However, ubiquitination of K63, but not K48 chains, was increased following XIAP^{NLS-C-term} overexpression (Figure 6), pointing to nuclear signaling transduction. Consistently, multivariate analysis found nuclear, but not cytoplasmic XIAP, as an independent prognostic factor in hormone receptor-negative breast cancer patients (Figure 7 and 8, Table 1). Altogether, our findings suggest that nuclear XIAP associates with poor outcome and RING-dependent breast cancer growth and chemoresistance.

Keywords: Breast cancer; Evasion from apoptosis; XIAP subcellular localization; Drug resistance; Prognosis

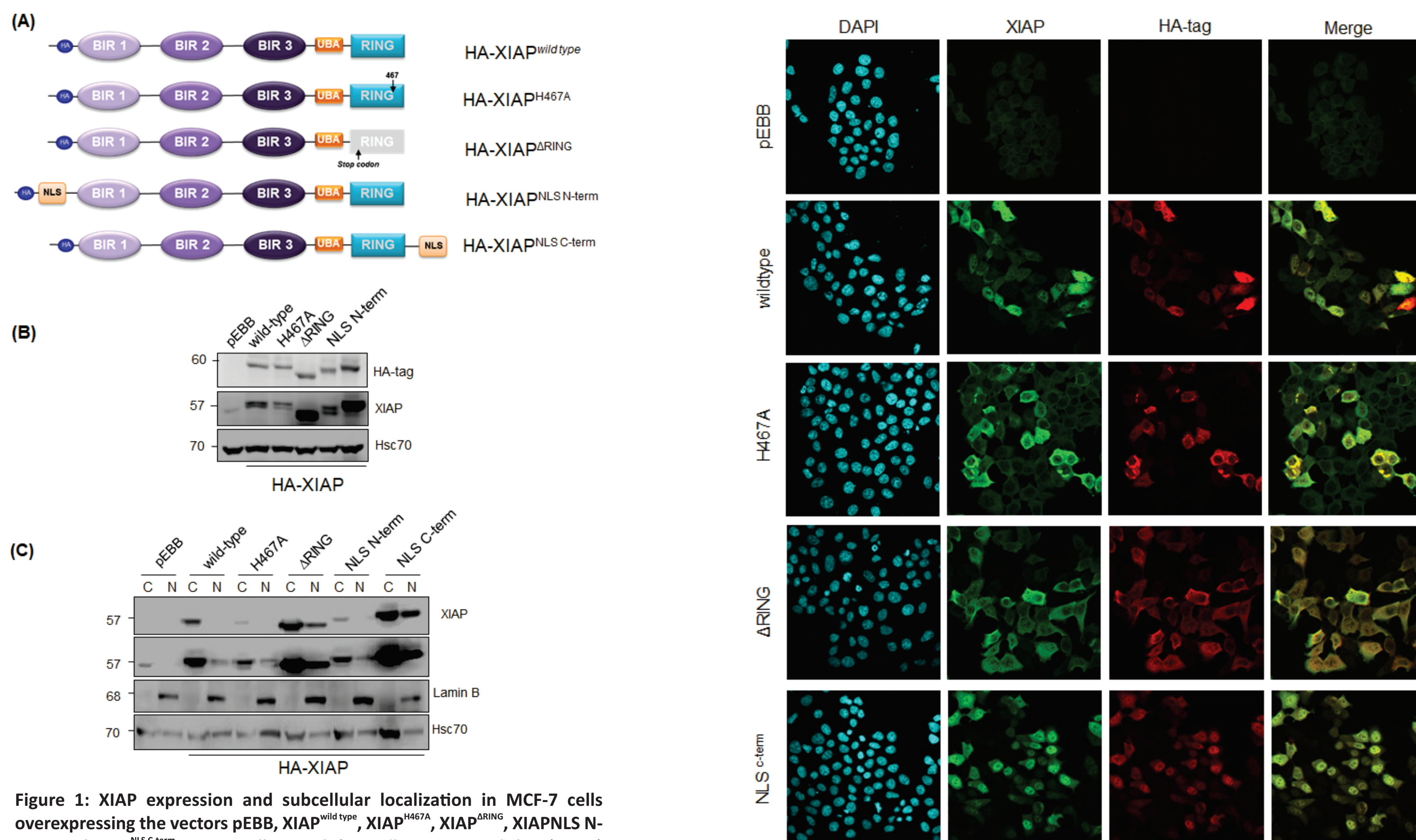


Figure 1: XIAP expression and subcellular localization in MCF-7 cells overexpressing the vectors pEBB, XIAP^{wild-type}, XIAP^{H467A}, XIAP^{ΔRING}, XIAP^{NLS N-term} and XIAP^{NLS C-term}. MCF-7 cells were left to adhere in petri dishes (10cm) for 24 h and thereafter, were transfected with the pEBB, XIAP^{wild-type}, XIAP^{H467A}, XIAP^{ΔRING}, XIAP^{NLS N-term} and XIAP^{NLS C-term} vectors (A), using Lipofectamine 2000. (B) The levels of XIAP expression in XIAP-transfected cells were examined by Western blotting. (C) MCF-7 cells had their cytoplasmic and nuclear fractions separated by NE-PER kit (ThermoScientific). XIAP expression was evaluated by Western blotting. Lamin B was used as a nuclear constitutive control, while Hsc70, as cytoplasmic constitutive control. C: cytoplasm; N: nucleus.

Figure 2: Confocal analysis of XIAP subcellular localization in MCF-7 cells overexpressing the vectors pEBB, XIAP^{wild-type}, XIAP^{H467A}, XIAP^{ΔRING} and XIAP^{NLS C-term}. MCF-7 cells were left to adhere for 24 h and thereafter, were transfected with the pEBB, XIAP^{wild-type}, XIAP^{H467A}, XIAP^{ΔRING} and XIAP^{NLS C-term} vectors (A), using Lipofectamine 2000. Cells were then fixed and labelled with anti-XIAP and anti-HA-tag antibodies, prior to immuno-fluorescence analysis. Nuclei were counterstained with DAPI.

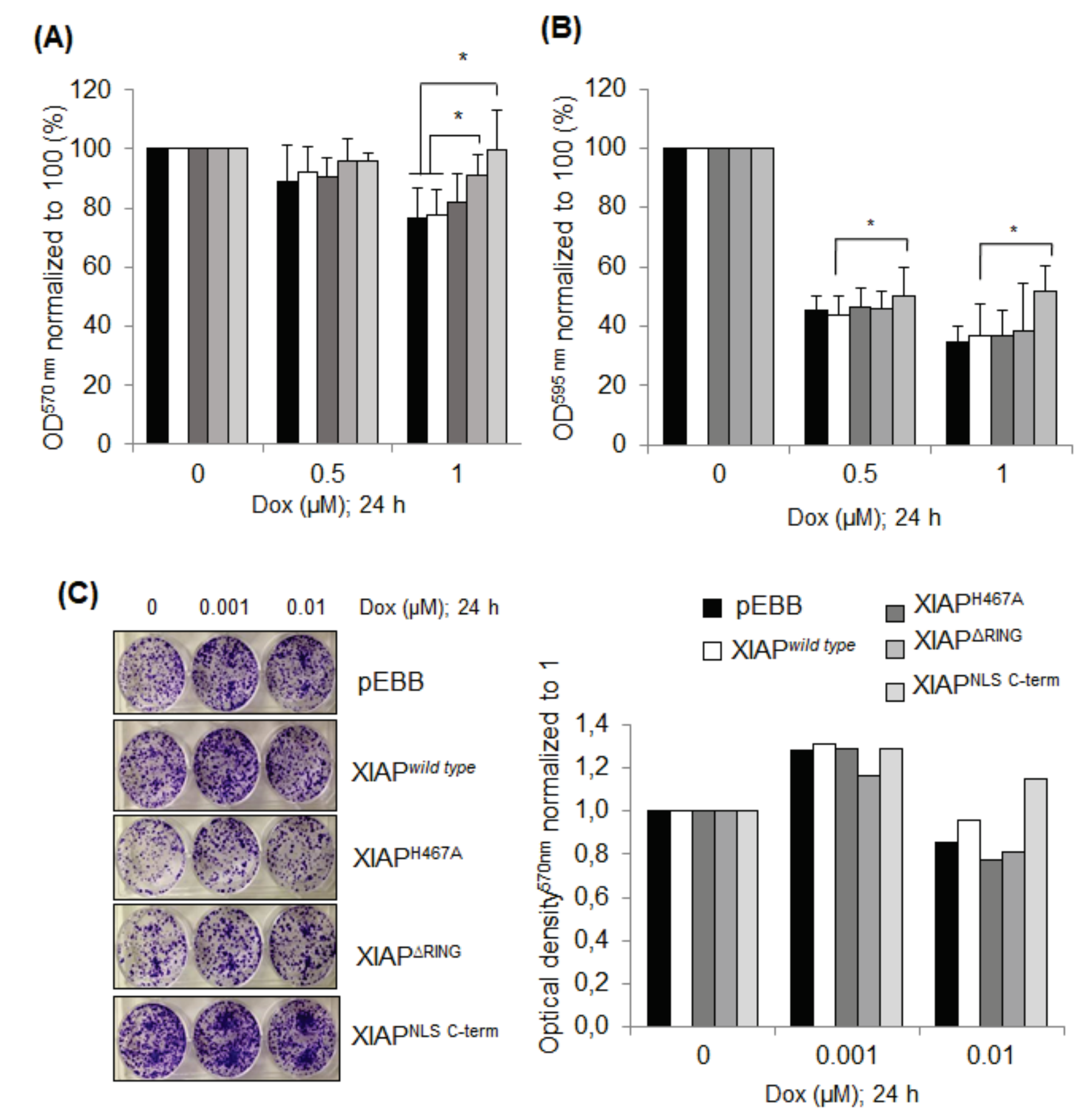


Figure 3: Effect of overexpression of XIAP and its mutants on doxorubicin (dox) resistance in breast cancer cells. MCF-7 cells were left to adhere in petri dishes (10cm) or, alternatively, in 6-well plates for 24 h and thereafter, were transfected with the vectors pEBB, XIAP^{wild-type}, XIAP^{H467A}, XIAP^{ΔRING} and XIAP^{NLS C-term}, using Lipofectamine 2000. After 24 h of transfection, MCF-7 cells were left to adhere in 96-well plates for 24 h. Subsequently, dox was added at 0,5 e 1 μM concentrations and the cells were incubated for 24 h for MTT (A) and for 72 h for crystal violet assays (B). Optical density was obtained at 570 nm and 595 nm, respectively. For each dox concentration, the cell lines transfected with the different XIAP-encoding plasmids were compared to the XIAP wild-type transfected cells and to the empty vector pEBB. The graphs correspond to means and standard deviation of three independent experiments (Student t test: * p < 0.05, considered statistically significant). (C) After 24 h of transfection, MCF-7 cells were left to adhere in 6-well plates for 24 h. On the following day, cells were treated with dox for 24 h. After colony formation, cells were stained with crystal violet and had their viability measured at 595nm. The graph is representative of three independent experiments.

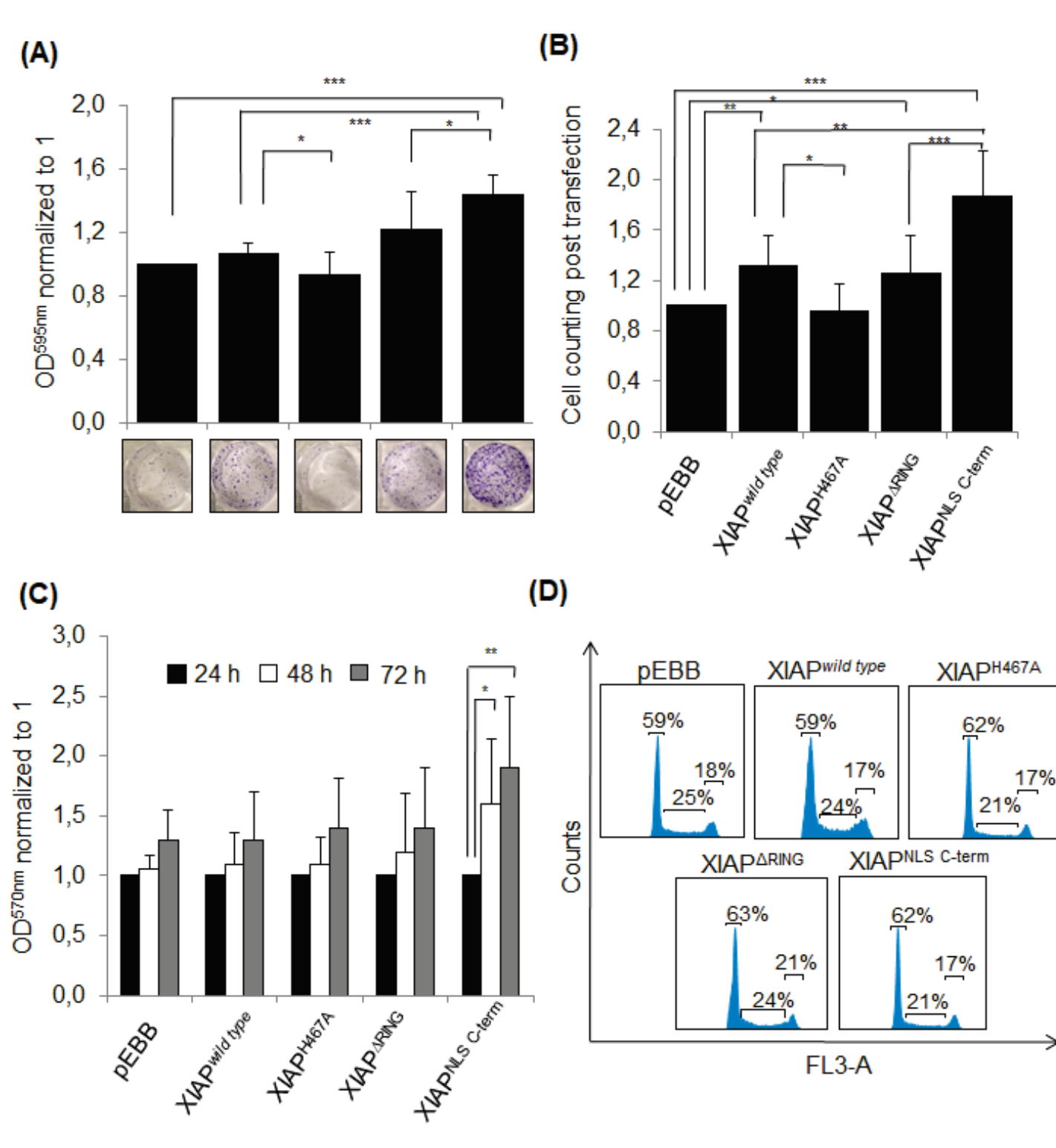


Figure 4: Effect of overexpression of XIAP and its mutants on cell growth of breast cancer cells. MCF-7 cells were left to adhere in petri dishes (10cm) or, alternatively, in 6-well plates for 24 h and thereafter, were transfected with the pEBB, XIAP^{wild-type}, XIAP^{H467A}, XIAP^{ΔRING} and XIAP^{NLS C-term} vectors using Lipofectamine 2000. (A) After 24 h of transfection, MCF-7 cells were left to adhere in 6-well plates for 24 h. After colony formation, cells were stained with crystal violet and had their viability measured at 595 nm. The graph corresponds to the mean and standard deviation of four independent experiments (Student t test: * p < 0.05; ** p < 0.01; *** p < 0.001; considered statistically significant). (B) Transfected cells were counted via trypan blue exclusion 24 h post transfection. The total number of cells transfected with the empty vector (pEBB) each experiment was normalized to the value of 1. The graph corresponds to means and standard deviation of five independent experiments (Student's t test: * p < 0.05; considered statistically significant). (C) Cells were transfected and left to adhere in 96-well plate. Cell mitochondrial viability was assessed following 24, 48 and 72 h after dox treatment. Optical density was obtained at 570 nm. (D) The cell cycle profile of XIAP-overexpressing cells was evaluated by flow cytometry analysis of DNA content. The histograms are representative of three independent experiments.

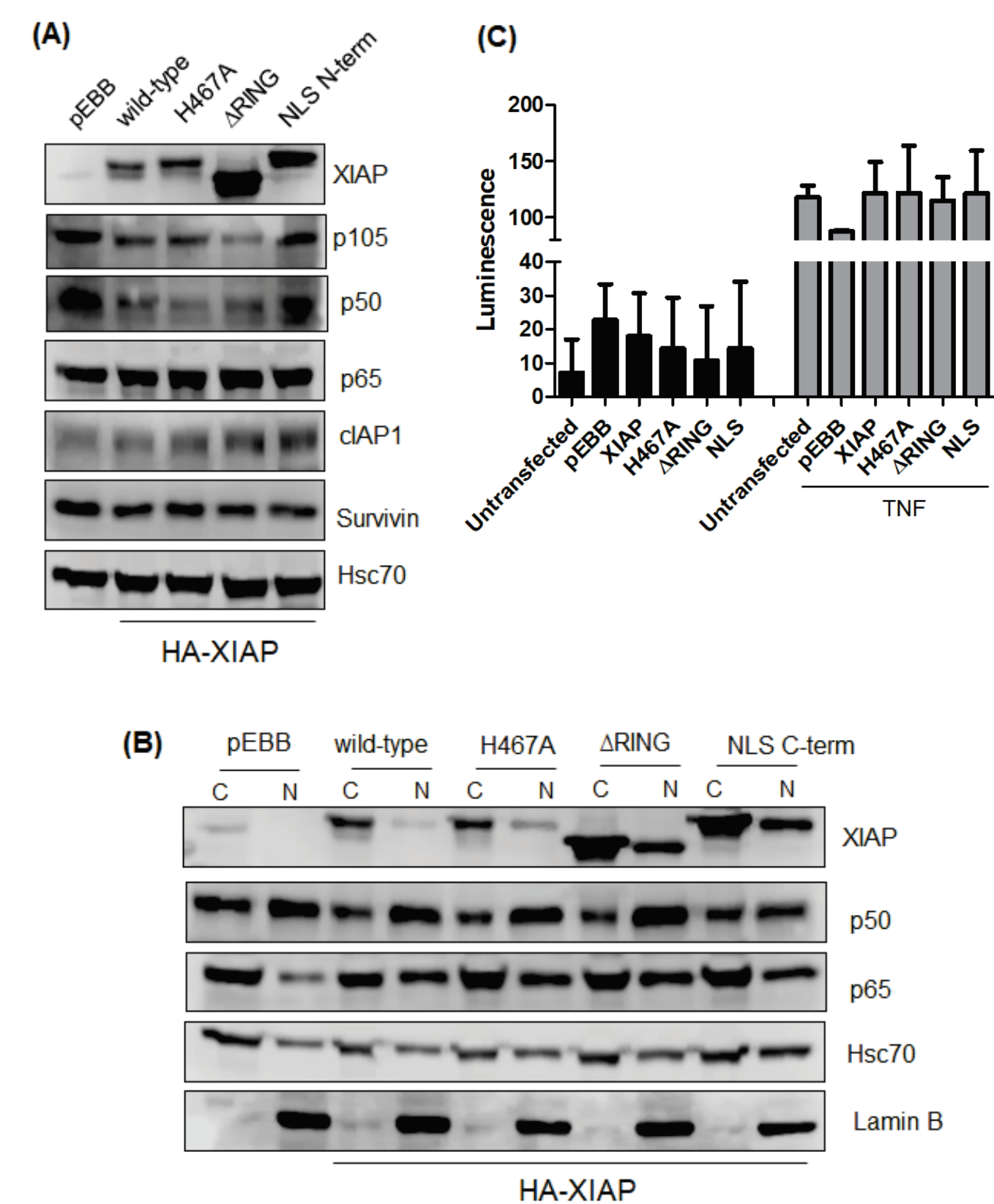


Figure 5: Expression pattern of NFκB subunits, cIAP1 and Survivin following overexpression of XIAP and its mutants in breast cancer cells. MCF-7 cells were left to adhere in petri dishes (10cm) for 24 h and thereafter, were transfected with the pEBB, XIAP^{wild-type}, XIAP^{H467A}, XIAP^{ΔRING}, XIAP^{NLS N-term} and XIAP^{NLS C-term} vectors, using Lipofectamine 2000. The expression levels of XIAP, NFκB subunits (p50, p105 and p65), cIAP1 and Survivin in XIAP-transfected cells were examined in whole cell (A) and fractionated lysates (B) by Western blotting. Hsc70 was used as a constitutive control. Lamin B was used as a nuclear constitutive control. C: Cytoplasm; N: Nucleus (C) NFκB transcriptional activity was assessed by luciferin-luciferase assay.

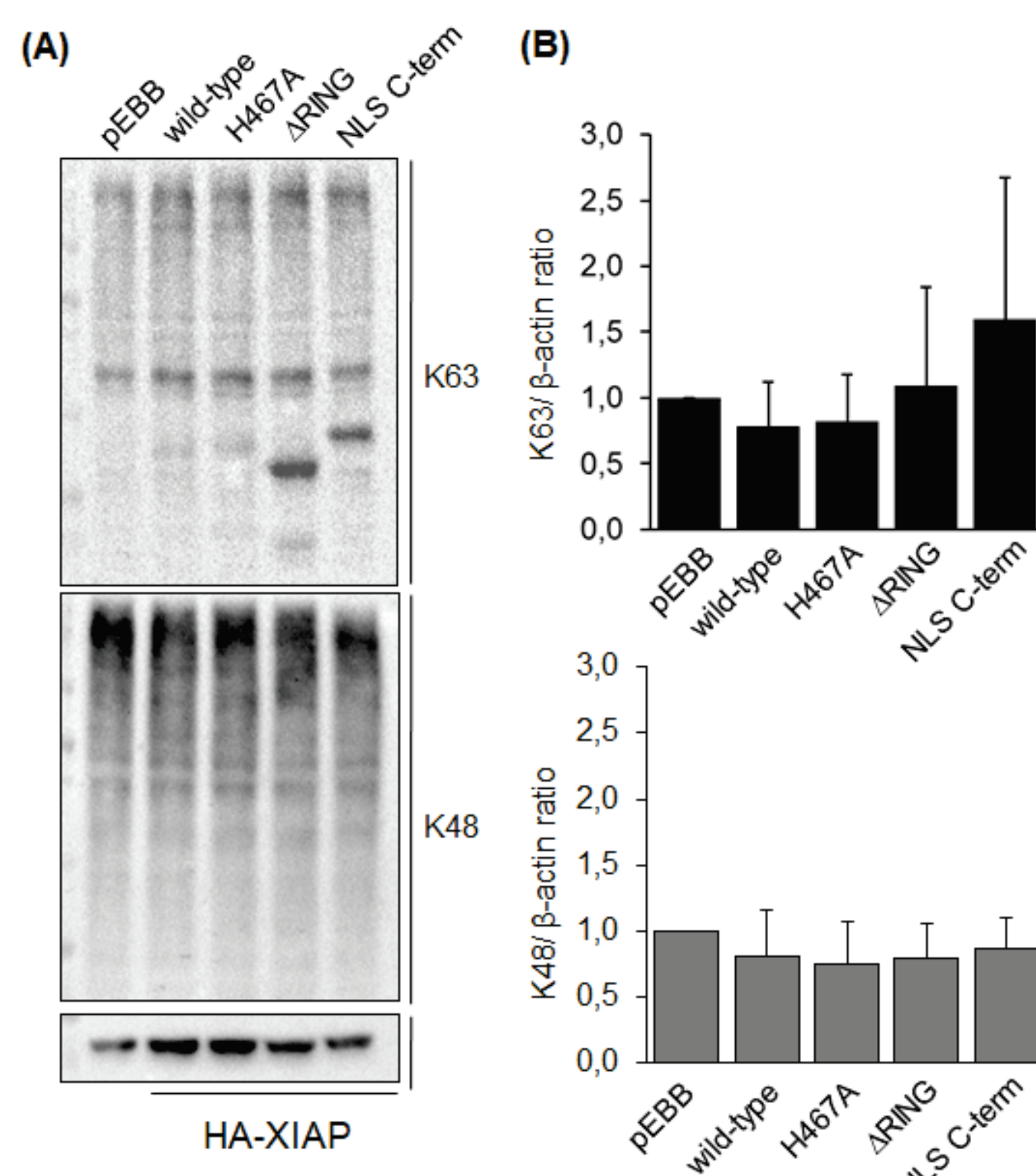


Figure 6: Overexpression of mutant forms of XIAP is associated with an increase in K63, but not K48-linked ubiquitination. MCF-7 cells were left to adhere in petri dishes (10cm) for 24 h and thereafter, were transfected with the pEBB, XIAP^{wild-type}, XIAP^{H467A}, XIAP^{ΔRING}, XIAP^{NLS N-term} and XIAP^{NLS C-term} vectors, using Lipofectamine 2000. The expression pattern of K63 and K48 ubiquitin chains were measured by Western blotting using K63 and K48-specific antibodies (A) and quantification was performed following normalization against β-actin levels (B).

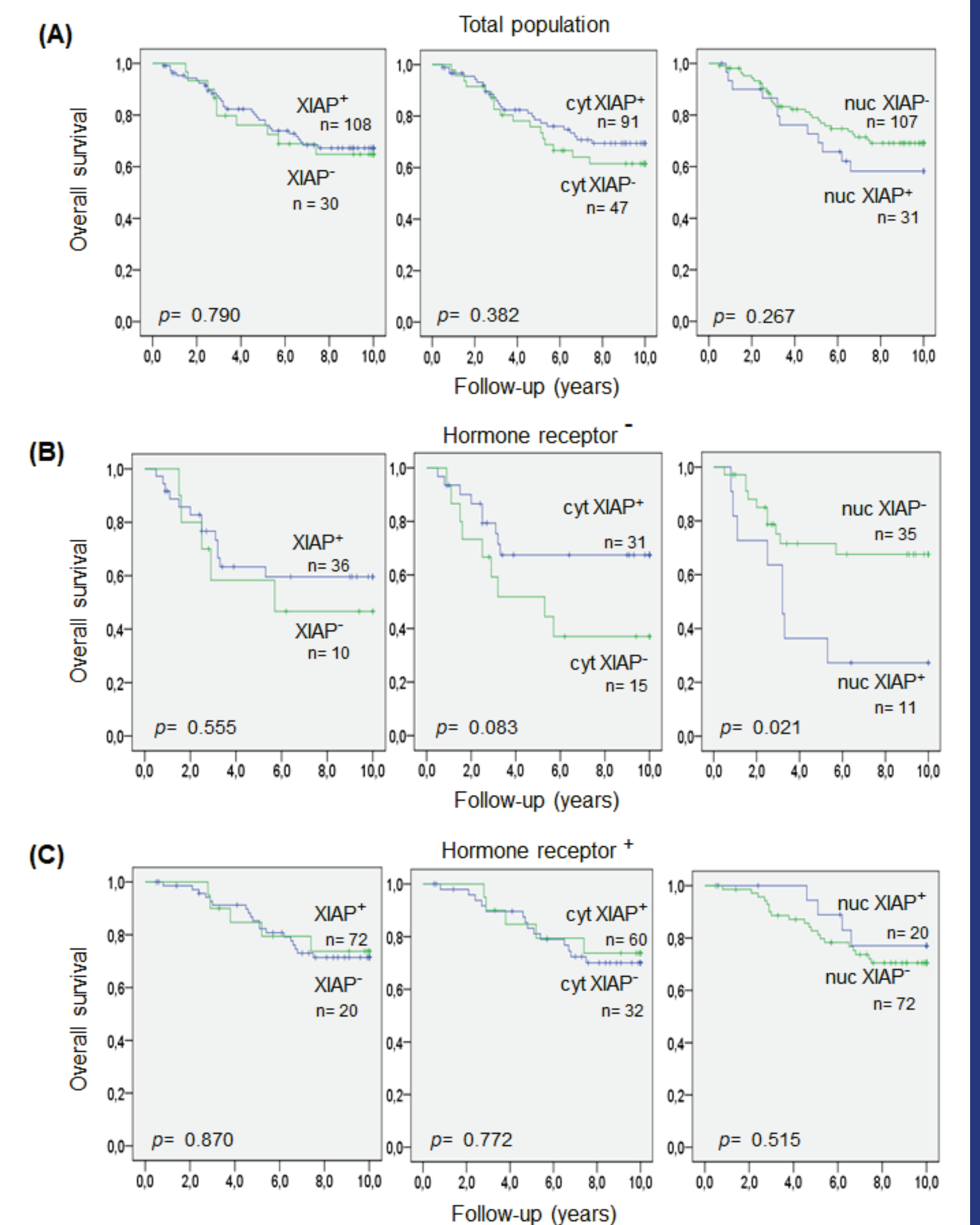


Figure 7: Overall survival of patients with infiltrating ductal breast carcinoma grouped according to total, cytoplasmic or nuclear expression of XIAP. The impact of XIAP expression and subcellular localization was analyzed in the total population (A) and in hormone receptor-negative (B) and positive (C) subgroups. The Kaplan-Meier curves were compared by the log-rank test, where the value of p < 0.05 was considered statistically significant. HR: Hormone Receptors; Cyt: cytoplasmic; Nuc: Nuclear.

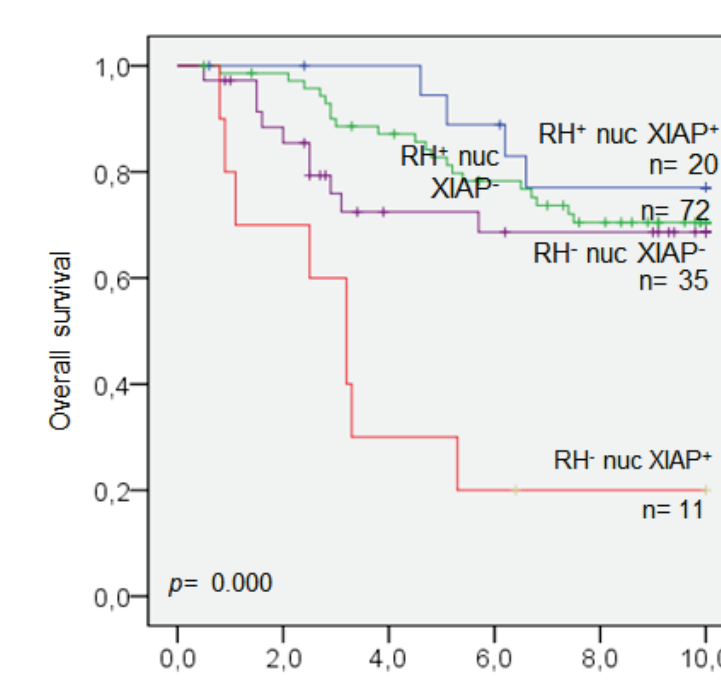


Figure 8: Overall survival of patients with infiltrating ductal breast carcinoma grouped according to XIAP subcellular localization and expression of hormone receptors. The impact of XIAP subcellular localization and expression of hormone receptors was analyzed in the total population following stratification. The Kaplan-Meier curves were compared by the log-rank test, where the value of p < 0.05 was considered statistically significant. HR: Hormone Receptors; Nuc: Nuclear.

Table 1: Multivariate analysis of XIAP expression and localization and breast cancer prognostic factors

Characteristics	Total population			Hormone receptor-positive patients			Hormone receptor-negative patients		
	p	HR	(95% CI)	p	HR	(95% CI)	p	HR	(95% CI)
Age at diagnosis	0.814	0.055	(0.964 - 1.048)	0.569	0.569	(0.933 - 1.039)	0.409	0.682	(0.957 - 1.114)
Tumor size	0.631	0.231	(0.583 - 1.396)	0.767	0.088	(0.640 - 1.389)	0.206	1.600	(0.181 - 1.446)
Tumor grade	0.340	0.912	(0.686 - 2.987)	0.498	0.459	(0.504 - 4.089)	0.061	3.497	(0.910 - 55.629)
Her2 expression	0.161	1.964	(0.556 - 34.298)	0.986	0.000	(0.000 -)	0.560	0.340	(0.184 - 22.867)
Hormone receptors	0.023	5.167	(1.140 - 5.878)	-	-	-	-	-	-
Total XIAP expression	0.756	0.097	(0.264 - 6.333)	0.406	0.691	(0.024 - 4.503)	0.326	0.966	(0.223 - 92.968)
Cytoplasmic XIAP	0.720	0.128	(0.334 - 4.894)	0.554	0.351	(0.198 - 20.574)	0.669	0.183	(0.174 - 15.216)
Nuclear XIAP	0.358	0.846	(0.175 - 1.875)	0.567	0.328	(0.231 - 14.459)	0.011	6.504	(0.004 - 4.483)

p < 0.05; statistically significant; HR: Hazard ratio; CI: Confidence interval